Electronic Supplementary Information for

Heavy Atom Tunneling in the Automerization of Pentalene and other Antiaromatic Systems

S. Kozuch

Page

SCT calculations on cyclobutadiene S2

*t*Bu$_3$PL conformers S3

Benchmark study of DFT methods for PL and HL automerization ... S4

^{12}C/^{13}C Kinetic isotope effect on PL S3

XYZ Geometries S5

Polyrate Outputs S7

SCT Calculations on Cyclobutadiene (CBD):

Since the transition state for the automerization of **CBD** is an open-shell singlet diradical, unrestricted (u)DFT was employed on it. uDFT is not an accurate method for this system, giving a wave function contaminated by a triplet state, when ideally requires a multireference method for its correct description. However, the $\Delta E^{\ddagger}$ obtained with uM06-2X/6-31G(d) was 7.0 kcal/mol, close to the best estimate of 9 kcal mol^{-1}.[1] It must be noted that this underestimation of $\Delta E^{\ddagger}$ also results in an underestimation of the barrier width (the most significant factor for a fast QMT),[2] and therefore the calculated rate constant for tunnelling in the automerization of **CBD** will be overestimated, but will still serve us as a qualitative upper bound.

Carpenter estimated the tunneling rate constant of **CBD** at 223 K as 8×10^4 s^{-1}, almost three orders of magnitude faster than the classical value.[3] Even at 0 °C the tunneling was calculated to be responsible for more than 97% of the automerization. The experimental polarized IR spectrum of **CBD** at cryogenic temperatures confirmed a fast bond shifting with a rate higher than 10^3 s^{-1}.[4] Since the reaction was carried out in an Ar matrix, this value is estimated to be a lower bound of the ideal gas phase rate. Subsequent theoretical calculations by different methodologies set the rate to higher values of 2×10^{11}, 5×10^{11}, 2×10^{11} and 3×10^8 s^{-1} (calculated at different conditions, see refs. 5, 6, 7 and 8, respectively). Clearly it is not an easy value to compute, and the instability of this species does not help to determine it experimentally. Nonetheless, even in the most conservative estimations, the heavy atom tunneling is confirmed.

Table S1: uM06-2X/6-31G(d) activation energies, CVT and SCT rate constants (s^{-1}) for the automerization reactions of **CBD** at selected temperatures.

T(K)	CVT	SCT
10	2.4×10^{-75}	4.8×10^{7}
50	6.7×10^{-6}	4.8×10^{7}
100	5.2×10^{3}	4.9×10^{7}
150	5.8×10^{6}	8.4×10^{7}
200	2.2×10^{8}	4.8×10^{8}
300	9.5×10^{9}	1.1×10^{10}
400	7.1×10^{10}	7.3×10^{10}

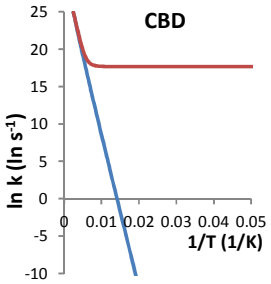

Fig. S1: Arrhenius plot for the **CBD** automerization.

In the SCT calculation provided here, the rate constant at temperatures lower than 100 K is 4.8×10^7 s^{-1}. However, as explained before, this is most probably an overestimation caused by an underestimation of the barrier by the unrestricted DFT methodology. The open-shell singlet TS calculated with M06-2X/6-31G(d) falls 2 kcal/mol short of the "best-estimate".[1] Therefore, the previous theoretical estimations setting the rate constant to ~10^{11} s^{-1} (refs. 5, 6 and 7) are also probably overshooting.

That said, the high SCT rate constant validate the fact that **CBD** can swiftly automerize by QMT from the ground state (see Table S1 and Fig. S1). However, the SCT results are at odds with the claim that at 0 °C there is still significant tunneling,[3] and further calculations with more accurate quantum chemical methods are required to solve this issue.

A significant difference between **CBD** and **PL** is that even at high temperatures bond shifting in the latter is calculated to proceed by tunneling from vibrationally excited states. The reason for this difference between the two systems resides in the comparison between their barrier heights and widths. Fig. S2 shows the energy of the system vs. the displacement of the carbon atoms with the wider trajectory. It is possible to see that the barrier profile for **PL** is higher but narrower than for **CBD**. The activation energy is a factor that affects both the "over the top" and the tunneling probability of crossing the barrier, but the width only affects the QMT. As a result, the narrower trajectory of the **PL** atoms compared to **CBD** will produce a larger SCT/CVT ratio, and **PL** will have a faster rate constant than **CBD**, in spite of its higher $\Delta E^{\ddagger}$. In Fig. S2 the critical bond distances are depicted, showing that the difference in bond length for single and double bonds of **PL** and **CBD** is significant (0.151 vs. 0.239 Å), explaining the distinct width of the barriers.

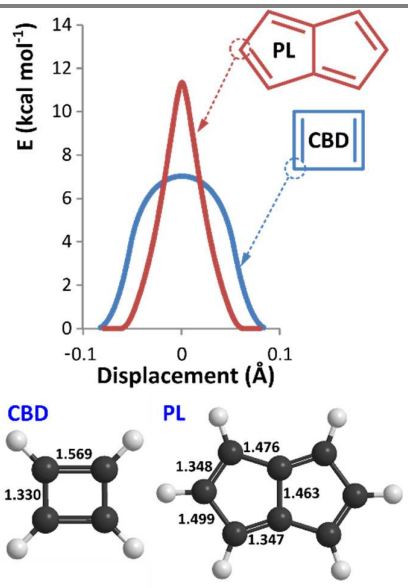

Fig. S2: Displacement graph for **CBD** and **PL**.

1. D. I. Lyakh, V. F. Lotrich, and R. J. Bartlett, *Chem. Phys. Lett.*, 2011, **501**, 166–171.
2. R. P. Bell, *The tunnel effect in chemistry*, Chapman and Hall, London; New York, 1980.
3. B. K. Carpenter, *J. Am. Chem. Soc.*, 1983, **105**, 1700–1701.
4. A. M. Orendt, B. R. Arnold, J. G. Radziszewski, J. C. Facelli, K. D. Malsch, H. Strub, D. M. Grant, and J. Michl, *J. Am. Chem. Soc.*, 1988, **110**, 2648–2650.
5. M. J. Huang and M. Wolfsberg, *J. Am. Chem. Soc.*, 1984, **106**, 4039–4040.
6. M. J. S. Dewar, K. M. Merz, and J. J. P. Stewart, *J. Am. Chem. Soc.*, 1984, **106**, 4040–4041.
7. P. Čársky, R. J. Bartlett, G. Fitzgerald, J. Noga, and V. Špirko, *J. Chem. Phys.*, 1988, **89**, 3008–3015.
8. R. Lefebvre and N. Moiseyev, *J. Am. Chem. Soc.*, 1990, **112**, 5052–5054.

Conformational analysis of 1,3,5-tri-*tert*-Butyl-pentalene (*t*Bu$_3$PL):

Me$_3$PL has only one stable conformer, with all the Me groups having a C-H eclipsing a π bond. ***t*Bu$_3$PL** global minimum geometry has the same conformation, but there are other higher energy stable conformers with C-C bonds in the *t*Bu groups anti to the double bonds (with almost negligible activation energy of rotation). We will label these conformers with a "+" for an eclipsing interaction, and a "-" for an anti conformation, in the order of substituents of Fig. S3.

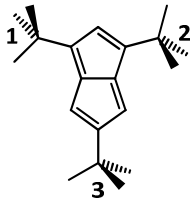

Fig. S3 "+ + +" conformer of ***t*Bu$_3$PL**.

Table S2 shows the energy of all the conformers (the unstable ones are optimized with fixed dihedral angles). It can be seen that each rotation requires an additive energy of ~2 kcal mol^{-1}, up to 6.5 kcal mol^{-1} for the unstable "- - -" geometry.

Table S2 Eight conformers of ***t*Bu$_3$PL**, their relative energies (in kcal mol^{-1}) and the local minimum connected to the unstable conformers.

Conformer	Rel *E*	Falls to
+ + +	0.0	
- + +	2.0	
+ + -	2.3	
+ - +	2.3	
- - + (unstable)	4.2	- + +
+ - - (unstable)	4.2	+ - +
- + - (unstable)	4.6	- + +
- - - (unstable)	6.5	- + +

The multiple minima situation generates multiple pathways and transition states for the bond shifting, connecting different conformers. Table S3 shows the four TS found for the degenerate rearrangement, and the reactant and product produced by following the IRC calculation. Transition state (a) is the lowest energy one, and the one described in the main text. Its conformation is similar to the TS of **Me$_3$PL**.

Table S3 Four possible transition states for the automerization of ***t*Bu$_3$PL**, with the connecting reactant and product conformers (note that these may not be stable, and can lead to other conformers, as shown in Table S2). Activation energies are in kcal mol^{-1}, taking as reference energy the global minimum conformer ("+ + +").

	TS	$\Delta E^{\ddagger}$	R	P
a	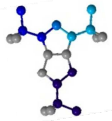	12.3	+ - -	- + +
b	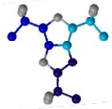	12.9	- + -	+ - +
c	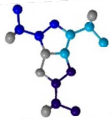	12.8	- - -	+ + +
d	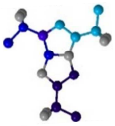	12.6	+ + -	- - +

Benchmark study of DFT methods for PL and HL automerization $\Delta E^{\ddagger}$. Absolute energies of the four species (C_{2h} and D_{2h} for PL, C_2 and D_2 for HL) in Ha, and relative energies ($\Delta E^{\ddagger}$) and errors in kcal mol^{-1}. All DFT calculations are with 6-31G(d).

Benchmark:
CCSD(T)-F12/CC-PVTZ-F12//M06-2X/6-311G(d)

PL		**HL**	
C2h	-307.91214	C2	-462.51771
D2h	-307.89408	D2	-462.49402
$\Delta E^{\ddagger}$	11.33	$\Delta E^{\ddagger}$	14.87

	B1B95	**B3LYP**	**B3PW91**	**B97D**	**B98**	**BB95**	**BLYP**	**BMK**	**BP86**	**M06-2X**
PL										
C_{2h}	-308.23078	-308.36891	-308.25223	-308.12760	-308.23986	-308.26497	-308.22870	-308.15030	-308.36269	-308.23076
D_{2h}	-308.21913	-308.35764	-308.24180	-308.12056	-308.22838	-308.25876	-308.22111	-308.13443	-308.35614	-308.21270
$\Delta E^{\ddagger}$	7.3	7.1	6.5	4.4	7.2	3.9	4.8	10.0	4.1	11.3
Error	4.0	4.3	4.8	6.9	4.1	7.4	6.6	1.4	7.2	0.0
HL										
C_2	-462.98607	-463.20899	-463.02958	-462.85671	-463.01317	-463.03405	-462.99072	-462.87288	-463.19470	-462.99844
D_2	-462.97478	-463.20096	-463.02115	-462.85398	-463.00446	-463.03209	-462.98918	-462.85796	-463.19301	-462.97775
$\Delta E^{\ddagger}$	7.1	5.0	5.3	1.7	5.5	1.2	1.0	9.4	1.1	13.0
Error	7.8	9.8	9.6	13.2	9.4	13.6	13.9	5.5	13.8	1.9
MUE	5.9	7.0	7.2	10.0	6.8	10.5	10.2	3.4	10.5	0.9

	M06	**M06-L**	**mPW1PW91**	**mPWPW91**	**PBE0**	**PBE**	**TPSSh**	**TPSS**	**ωB97XD**	**ωB97X**
PL										
C_{2h}	-308.32243	-308.12350	-308.29789	-308.32619	-308.00103	-307.97004	-308.39787	-308.43075	-308.25791	-308.28010
D_{2h}	-308.31550	-308.11277	-308.28662	-308.31970	-307.98995	-307.96378	-308.38891	-308.42365	-308.24182	-308.25998
$\Delta E^{\ddagger}$	4.3	6.7	7.1	4.1	7.0	3.9	5.6	4.5	10.1	12.6
Error	7.0	4.6	4.3	7.3	4.4	7.4	5.7	6.9	1.2	1.3
HL										
C_2	-462.83779	-463.13991	-463.09803	-463.13791	-462.65067	-462.60152	-463.24547	-463.29395	-463.04486	-463.07496
D_2	-462.82830	-463.13801	-463.08797	-463.13611	-462.64075	-462.59992	-463.23985	-463.29157	-463.02476	-463.04929
$\Delta E^{\ddagger}$	6.0	1.2	6.3	1.1	6.2	1.0	3.5	1.5	12.6	16.1
Error	8.9	13.7	8.6	13.7	8.6	13.9	11.3	13.4	2.3	1.2
MUE	7.9	9.1	6.4	10.5	6.5	10.6	8.5	10.1	1.7	1.3

^{12}C/^{13}C Kinetic isotope effect on the different monosubstitutions and complete isotopic substitution on PL (note that the use of ^{13}C on all the positions has a KIE almost equal to the product of the KIE of all the individual substitutions).

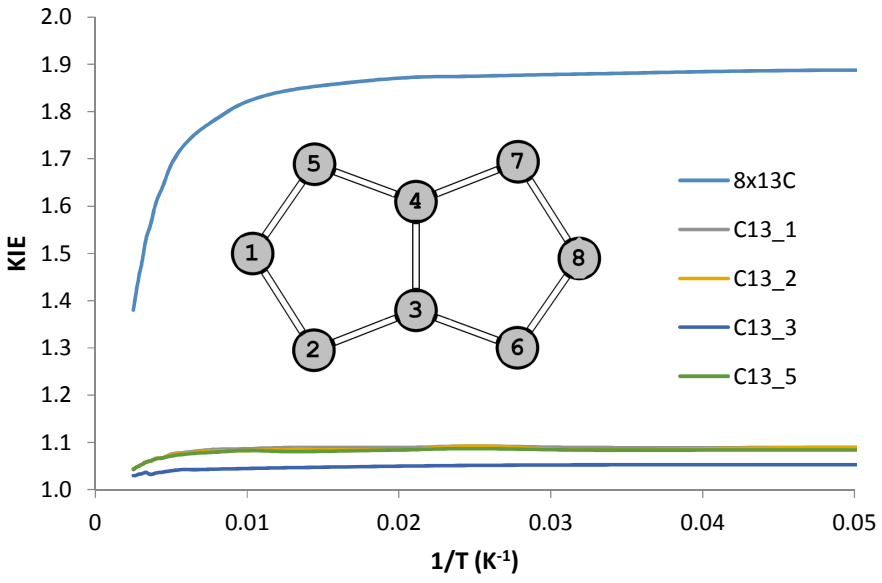

XYZ Geometries:

14
PL React
C 2.164684 -0.059040 0.000000
C 1.406669 -1.173902 0.000000
C -0.001420 -0.731616 0.000000
C 0.001420 0.731616 0.000000
C 1.281223 1.151928 0.000000
C -1.281223 -1.151928 0.000000
C -2.164684 0.059040 0.000000
C -1.406669 1.173902 0.000000
H 3.246917 -0.016514 0.000000
H 1.756566 -2.197628 0.000000
H 1.650505 2.171475 0.000000
H -1.650505 -2.171475 0.000000
H -3.246917 0.016514 0.000000
H -1.756566 2.197628 0.000000

14
PL TS
C 2.182502 0.000000 0.000000
C 1.350319 -1.137963 0.000000
C 0.000000 -0.704328 0.000000
C 0.000000 0.704328 0.000000
C 1.350319 1.137963 0.000000
C -1.350319 -1.137963 0.000000
C -2.182502 0.000000 0.000000
C -1.350319 1.137963 0.000000
H 3.262990 0.000000 0.000000
H 1.702346 -2.164502 0.000000
H 1.702346 2.164502 0.000000
H -1.702346 -2.164503 0.000000
H -3.262990 0.000000 0.000000
H -1.702346 2.164503 0.000000

23
Me3PL React
C 1.453052 1.124317 0.000000
C 1.743306 -2.619437 -0.000002
C 0.027173 0.713012 0.000002
C 1.943772 2.533340 0.000000
H -1.826483 -2.146065 0.000003
C 2.166249 -0.020324 -0.000001
H 3.248935 -0.097256 -0.000002
C -2.166161 0.001221 0.000000
C -1.236505 1.178753 0.000000
C -0.018038 -0.745410 0.000003
H -1.574413 2.210739 -0.000003
C 1.249574 -1.212722 0.000000
C -3.654788 0.138157 -0.000002
H 1.579186 3.073963 -0.880820
H 3.035785 2.571744 -0.000001
H 1.579188 3.073963 0.880820
C -1.433150 -1.136693 0.000002
H 2.368882 -2.809151 0.880223
H 2.368879 -2.809149 -0.880229
H 0.917183 -3.333853 -0.000001
H -4.002313 0.690577 -0.881052
H -4.002316 0.690574 0.881049
H -4.139417 -0.841360 -0.000004

23
Me3PL TS
C 0.002630 -1.365268 1.146331
C 0.001048 -1.845288 -2.557581
C -0.025449 -0.009527 0.704063
C 0.001048 -1.845288 2.557581
H 0.017819 1.695374 -2.162448
C 0.017199 -2.188388 0.000000
H 0.032429 -3.270878 0.000000
C 0.010014 2.175557 0.000000
C 0.001048 1.336734 1.136914
C -0.025449 -0.009527 -0.704063
H 0.017819 1.695374 2.162448
C 0.002630 -1.365268 -1.146331
C 0.005237 3.676838 0.000000
H 0.784595 -1.345493 3.136529
H 0.149976 -2.925365 2.617536
H -0.953744 -1.599769 3.037167
C 0.001048 1.336734 -1.136914
H 0.149976 -2.925365 -2.617536
H 0.784595 -1.345493 -3.136529
H -0.953744 -1.599769 -3.037167
H 0.517273 4.073140 0.882383
H -1.010294 4.091259 0.000000
H 0.517273 4.073140 -0.882383

14
Br3PL React
C 0.037740 0.000000 2.208692
C -1.154235 0.000000 1.309057
C -0.763716 0.000000 0.019014
C 0.694067 0.000000 0.019751
C 1.131430 0.000000 1.425398
C -1.215636 0.000000 -1.372120
C -0.087000 0.000000 -2.113539
C 1.130580 0.000000 -1.252378
H -0.011525 0.000000 3.288516
Br -2.888528 0.000000 1.972146
Br 2.912412 0.000000 1.952918
H -2.234910 0.000000 -1.730807
Br 0.025107 0.000000 -3.977333
H 2.144560 0.000000 -1.633197

14
Br3PL TS
C 0.000000 0.000000 2.232339
C -1.118721 0.000000 1.380180
C -0.705110 0.000000 0.025492
C 0.705110 0.000000 0.025492
C 1.118721 0.000000 1.380180
C -1.151045 0.000000 -1.314157
C 0.000000 0.000000 -2.122989
C 1.151045 0.000000 -1.314157
H 0.000000 0.000000 3.310975
Br -2.872857 0.000000 1.965793
Br 2.872857 0.000000 1.965793
H -2.171759 0.000000 -1.677449
Br 0.000000 0.000000 -3.997538
H 2.171759 0.000000 -1.677449

8
CBD React
C -0.784673 0.664996 0.000000
C -0.784673 -0.664996 0.000000
H 1.545681 1.435215 0.000000
H -1.545681 1.435215 0.000000
H 1.545681 -1.435215 0.000000
H -1.545681 -1.435215 0.000000
C 0.784673 0.664996 0.000000
C 0.784673 -0.664996 0.000000

8
CBD TS
C -0.719264 0.719264 0.000000
C -0.719264 -0.719264 0.000000
H 1.483360 1.483360 0.000000
H -1.483360 1.483360 0.000000
H 1.483360 -1.483360 0.000000
H -1.483360 -1.483360 0.000000
C 0.719264 0.719264 0.000000
C 0.719264 -0.719264 0.000000

22
HL React
C 2.979971 0.098862 0.402375
C 2.352666 -1.062993 0.685104
C 2.470844 1.152335 -0.455613
H 3.221692 1.805281 -0.896722
H 3.990728 0.234288 0.778947
H 0.905899 -2.573728 0.184019
C 1.056133 -1.494991 0.207182
H 2.901033 -1.796978 1.271717
H 0.978715 2.239452 -1.431325
H -0.978715 -2.239452 -1.431325
C -1.056133 1.494991 0.207182
C 1.185222 1.415684 -0.750079
C -2.352666 1.062993 0.685104
C -0.005123 0.739706 -0.189521
H -0.905899 2.573728 0.184019
C 0.005123 -0.739706 -0.189521
H -2.901033 1.796978 1.271717
C -1.185222 -1.415684 -0.750079
C -2.470844 -1.152335 -0.455613
C -2.979971 -0.098862 0.402375
H -3.221692 -1.805281 -0.896722
H -3.990728 -0.234288 0.778947

22
HL TS

C	3.196783	0.000000	0.000000
C	2.534047	-1.205453	0.211687
C	2.534047	1.205453	-0.211687
H	3.172285	2.069286	-0.392430
H	4.280714	0.000000	0.000000
H	0.962235	-2.552340	0.376463
C	1.180405	-1.501514	0.207138
H	3.172285	-2.069286	0.392430
H	0.962235	2.552340	-0.376463
H	-0.962235	-2.552340	-0.376463
C	-1.180405	1.501514	0.207138
C	1.180405	1.501514	-0.207138
C	-2.534047	1.205453	0.211687
C	0.000000	0.721883	0.000000
H	-0.962235	2.552340	0.376463
C	0.000000	-0.721883	0.000000
H	-3.172285	2.069286	0.392430
C	-1.180405	-1.501514	-0.207138
C	-2.534047	-1.205453	-0.211687
C	-3.196783	0.000000	0.000000
H	-3.172285	-2.069286	-0.392430
H	-4.280714	0.000000	0.000000

16
APL React

C	0.587889	-1.563246	1.416271
H	-0.635361	-0.459470	-2.931919
C	-0.018790	-0.524314	2.047642
H	0.317229	-2.552574	-1.611188
C	-0.135322	0.621935	1.083610
C	0.584704	0.269207	0.005332
C	0.832493	-1.154257	-0.002612
C	-1.043789	1.727620	0.626516
C	-0.956861	1.830684	-0.725479
C	-0.035667	0.753425	-1.206424
H	0.832413	-2.518484	1.863951
H	-0.349404	-0.524550	3.079653
C	0.467164	-1.538401	-1.254837
H	-1.658604	2.351506	1.264625
H	-1.477329	2.556067	-1.338363
C	-0.076530	-0.343738	-2.008697

16
APL TS

C	0.558938	-1.507602	1.216756
H	-0.716280	-0.594521	-2.800193
C	-0.143549	-0.483134	1.887808
H	0.532480	-2.553042	-1.514793
C	-0.034879	0.665982	1.079035
C	0.831365	0.361181	0.000000
C	1.141194	-1.013858	0.000000
C	-0.924336	1.823751	0.670195
C	-0.924336	1.823751	-0.670195
C	-0.034879	0.665982	-1.079035
H	0.532480	-2.553042	1.514793
H	-0.716280	-0.594521	2.800193
C	0.558938	-1.507602	-1.216756
H	-1.449874	2.498278	1.334549
H	-1.449874	2.498278	-1.334549
C	-0.143549	-0.483134	-1.887808

50
tBu3PL React

C	-1.323398	-1.193330	0.000093
C	-1.866901	2.599273	0.000013
C	-0.034538	-0.776692	-0.000573
C	-1.901820	-2.582539	0.000147
H	1.633529	2.118620	-0.000447
C	-2.188643	0.039294	0.000239
H	-3.272687	0.007263	0.000710
C	2.149551	-0.111813	-0.000203
C	1.369812	-1.219362	-0.000319
C	-0.021043	0.684378	-0.000758
H	1.718514	-2.243331	-0.000205
C	-1.432449	1.156818	-0.000299
C	3.655954	-0.018104	0.000124
C	-2.773536	-2.760611	-1.255106
C	-2.774243	-2.760875	1.254725
C	-0.794639	-3.637214	0.000305
H	-3.214508	-3.763877	-1.263394
C	1.261802	1.098041	-0.000427
H	-2.174982	-2.638944	-2.163545
H	-3.589880	-2.031908	-1.285499
H	-1.230370	-4.642206	0.000293
H	-0.161267	-3.538810	0.888273
H	-0.161139	-3.538897	-0.887586
H	-3.215266	-3.764126	1.262466
H	-3.590603	-2.032189	1.284877
H	-2.176299	-2.639544	2.163617
C	-1.308812	3.292766	-1.254145
C	-1.308222	3.292353	1.254222
C	-3.392708	2.709757	0.000502
H	-3.694332	3.762614	0.000502
H	-3.821041	2.233076	0.888695
H	-3.821621	2.232880	-0.887321
H	-1.593031	4.350641	1.259295
H	-0.216146	3.230636	1.288231
H	-1.700863	2.824089	2.162531
H	-1.593525	4.351082	-1.258772
H	-1.701767	2.824896	-2.162522
H	-0.216739	3.231021	-1.288646
C	4.116720	0.744247	-1.253430
C	4.287836	-1.411380	0.000339
C	4.116136	0.744341	1.253857
H	5.207978	0.840154	1.261439
H	3.808665	0.216329	2.162135
H	3.690725	1.753070	1.288066
H	5.380085	-1.330624	0.000432
H	3.988044	-1.978687	-0.887221
H	3.987891	-1.978512	0.887959
H	5.208552	0.840158	-1.260450
H	3.691176	1.752918	-1.287951
H	3.809743	0.216114	-2.161808

50
tBu3PL TS

C	-1.444975	-1.132433	0.000028
C	-1.835074	2.605728	-0.000057
C	-0.073729	-0.711980	0.000136
C	-1.937393	-2.554423	-0.000046
H	1.685722	2.122017	-0.000014
C	-2.241913	0.030652	-0.000048
H	-3.321972	0.054432	-0.000094
C	2.129672	-0.049004	0.000085
C	1.263397	-1.169529	0.000131
C	-0.047559	0.694718	0.000096
H	1.597242	-2.202830	0.000180
C	-1.395149	1.166264	-0.000005
C	3.645664	-0.048083	0.000071
C	-1.395647	-3.262381	1.255608
C	-1.395613	-3.262229	-1.255775
C	-3.466459	-2.625047	-0.000073
H	-1.738197	-4.303222	1.271025
C	1.310717	1.101513	0.000050
H	-1.751578	-2.767788	2.164923
H	-0.302273	-3.254982	1.272074
H	-3.790982	-3.670888	-0.000104
H	-3.884617	-2.139536	-0.887872
H	-3.884645	-2.139578	0.887736
H	-1.738234	-4.303044	-1.271371
H	-0.302236	-3.254900	-1.272164
H	-1.751450	-2.767471	-2.165036
C	-1.267050	3.293000	1.255604
C	-3.360487	2.732397	-0.000043
C	-1.267085	3.292885	-1.255799
H	-1.568514	4.346365	-1.269931
H	-1.642868	2.813593	-2.165287
H	-0.174846	3.242541	-1.273065
H	-3.647194	3.789243	-0.000066
H	-3.796116	2.262484	0.887758
H	-3.796138	2.262442	-0.887810
H	-1.568496	4.346476	1.269659
H	-0.174810	3.242676	1.272834
H	-1.642789	2.813780	2.165149
C	4.165114	0.678217	1.251353
C	4.165088	0.677673	-1.251540
C	4.186700	-1.480871	0.000377
H	5.281944	-1.471236	0.000401
H	3.853369	-2.029857	-0.887459
H	3.853318	-2.029491	0.888422
H	5.261425	0.700505	-1.260460
H	3.805794	1.712059	-1.283278
H	3.821249	0.174591	-2.161078
H	5.261452	0.700993	1.260269
H	3.821240	0.175579	2.161122
H	3.805892	1.712643	1.282612

Polyrate Outputs:

PL

T(K)	TST	CVT	CVT/ZCT	CVT/SCT
6	0.0E+00	0.0E+00	NaN	2.2E+08
8	3.0E-248	3.0E-248	1.4E+06	2.2E+08
10	2.1E-196	2.1E-196	1.4E+06	2.2E+08
20	1.3E-92	1.3E-92	1.4E+06	2.2E+08
30	6.2E-58	6.2E-58	1.4E+06	2.2E+08
40	1.5E-40	1.5E-40	1.5E+06	2.3E+08
50	4.2E-30	4.2E-30	1.5E+06	2.3E+08
75	4.2E-16	4.2E-16	1.9E+06	2.7E+08
100	4.7E-09	4.7E-09	2.7E+06	3.3E+08
125	8.4E-05	8.4E-05	4.1E+06	4.1E+08
150	5.9E-02	5.9E-02	6.7E+06	5.2E+08
175	6.6E+00	6.6E+00	1.1E+07	6.6E+08
200	2.3E+02	2.3E+02	2.0E+07	8.6E+08
225	3.7E+03	3.7E+03	3.5E+07	1.1E+09
250	3.5E+04	3.5E+04	6.3E+07	1.5E+09
275	2.2E+05	2.2E+05	1.1E+08	1.9E+09
300	1.0E+06	1.0E+06	1.9E+08	2.5E+09
325	3.7E+06	3.7E+06	3.3E+08	3.4E+09
350	1.1E+07	1.1E+07	5.5E+08	4.4E+09
375	3.0E+07	3.0E+07	8.8E+08	5.8E+09
400	7.0E+07	7.0E+07	1.4E+09	7.6E+09

CBD

T(K)	TST	CVT	CVT/ZCT	CVT/SCT
6	7.6E-133	7.6E-133	2.5E+07	4.8E+07
8	6.4E-97	6.4E-97	2.5E+07	4.8E+07
10	2.4E-75	2.4E-75	2.5E+07	4.8E+07
20	4.5E-32	4.5E-32	2.5E+07	4.8E+07
30	1.4E-17	1.4E-17	2.5E+07	4.8E+07
40	2.7E-10	2.7E-10	2.5E+07	4.8E+07
50	6.7E-06	6.7E-06	2.5E+07	4.8E+07
75	5.4E+00	5.4E+00	2.6E+07	4.8E+07
100	5.2E+03	5.2E+03	2.6E+07	4.9E+07
125	3.4E+05	3.4E+05	3.2E+07	5.6E+07
150	5.8E+06	5.8E+06	5.5E+07	8.4E+07
175	4.5E+07	4.5E+07	1.5E+08	1.8E+08
200	2.2E+08	2.2E+08	4.2E+08	4.8E+08
225	7.4E+08	7.4E+08	1.1E+09	1.2E+09
250	2.0E+09	2.0E+09	2.7E+09	2.8E+09
275	4.7E+09	4.7E+09	5.6E+09	5.8E+09
300	9.5E+09	9.5E+09	1.1E+10	1.1E+10
325	1.7E+10	1.7E+10	1.9E+10	1.9E+10
350	3.0E+10	3.0E+10	3.1E+10	3.2E+10
375	4.7E+10	4.7E+10	4.8E+10	4.9E+10
400	7.1E+10	7.1E+10	7.2E+10	7.3E+10

APL

T(K)	TST	CVT	CVT/ZCT	CVT/SCT
6	2.73E-218	2.7E-218	2.96E-15	1.9E-09
8	5.23E-161	5.2E-161	2.96E-15	1.9E-09
10	1.29E-126	1.3E-126	2.96E-15	1.9E-09
20	1.00E-57	1.0E-57	2.97E-15	1.9E-09
30	1.10E-34	1.1E-34	4.19E-15	2.2E-09
40	3.96E-23	4.0E-23	3.83E-14	5.6E-09
50	3.59E-16	3.6E-16	3.19E-12	5.0E-08
75	7.55E-07	7.6E-07	5.13E-06	1.5E-04
100	3.76E-02	3.8E-02	1.03E-01	3.4E-01
125	2.58E+01	2.6E+01	5.08E+01	9.1E+01
150	2.05E+03	2.1E+03	3.40E+03	4.9E+03
175	4.74E+04	4.7E+04	7.06E+04	9.1E+04
200	5.05E+05	5.1E+05	6.98E+05	8.4E+05
225	3.19E+06	3.2E+06	4.19E+06	4.9E+06
250	1.40E+07	1.4E+07	1.77E+07	2.0E+07
275	4.72E+07	4.7E+07	5.77E+07	6.4E+07
300	1.30E+08	1.3E+08	1.55E+08	1.7E+08
325	3.06E+08	3.1E+08	3.59E+08	3.9E+08
350	6.39E+08	6.4E+08	7.25E+08	7.7E+08
375	1.21E+09	1.2E+09	1.33E+09	1.4E+09
400	2.12E+09	2.1E+09	2.26E+09	2.4E+09

HL

T(K)	TST	CVT	CVT/ZCT	CVT/SCT
10	1.55E-240	1.55E-240	3.06E-52	1.2E-38
20	1.17E-114	1.17E-114	1.13E-39	3.6E-30
30	1.29E-72	1.29E-72	9.63E-27	4.4E-21
40	1.50E-51	1.50E-51	5.11E-19	8.5E-15
50	7.03E-39	7.03E-39	5.17E-14	1.4E-10
75	6.35E-22	6.35E-22	7.17E-07	1.8E-04
100	2.11E-13	2.11E-13	4.76E-03	3.6E-01
125	2.89E-08	2.89E-08	1.20E+00	4.3E+01
150	7.91E-05	7.91E-05	5.55E+01	1.2E+03
175	2.31E-02	2.31E-02	9.58E+02	1.4E+04
200	1.65E+00	1.65E+00	8.84E+03	9.5E+04
225	4.62E+01	4.62E+01	5.35E+04	4.4E+05
250	6.70E+02	6.70E+02	2.40E+05	1.6E+06
275	6.02E+03	6.02E+03	8.62E+05	4.8E+06
300	3.77E+04	3.77E+04	2.61E+06	1.2E+07
325	1.79E+05	1.79E+05	6.92E+06	2.8E+07
350	6.81E+05	6.81E+05	1.64E+07	5.8E+07
375	2.18E+06	2.18E+06	3.55E+07	1.1E+08
400	6.04E+06	6.04E+06	7.12E+07	2.0E+08

Br_3PL

T(K)	TST	CVT	CVT/ZCT	CVT/SCT
6	6.33E-250	6.33E-250	9.22E+05	2.8E+08
8	9.98E-185	9.98E-185	9.22E+05	2.8E+08
10	1.38E-145	1.38E-145	9.23E+05	2.8E+08
20	3.42E-67	3.42E-67	9.61E+05	2.9E+08
30	5.60E-41	5.60E-41	1.12E+06	3.1E+08
40	7.88E-28	7.88E-28	1.41E+06	3.5E+08
50	6.45E-20	6.45E-20	1.87E+06	3.9E+08
75	2.58E-09	2.58E-09	4.04E+06	5.5E+08
100	5.66E-04	5.66E-04	8.86E+06	7.9E+08
125	9.61E-01	9.61E-01	1.90E+07	1.1E+09
150	1.42E+02	1.42E+02	3.97E+07	1.6E+09
175	5.15E+03	5.15E+03	8.01E+07	2.2E+09
200	7.75E+04	7.75E+04	1.56E+08	3.0E+09
225	6.46E+05	6.46E+05	2.95E+08	4.1E+09
250	3.56E+06	3.56E+06	5.36E+08	5.5E+09
275	1.45E+07	1.45E+07	9.38E+08	7.5E+09
300	4.70E+07	4.70E+07	1.58E+09	1.0E+10
325	1.28E+08	1.28E+08	2.57E+09	1.3E+10
350	3.02E+08	3.02E+08	4.04E+09	1.8E+10
375	6.38E+08	6.38E+08	6.13E+09	2.3E+10
400	1.23E+09	1.23E+09	9.01E+09	3.0E+10

$^{57}H_3PL$

T(K)	TST	CVT	CVT/ZCT	CVT/SCT
6	0.00E+00	0.00E+00	NaN	NaN
8	8.34E-248	8.34E-248	2.17E+05	8.81E+07
10	4.76E-196	4.76E-196	2.17E+05	8.81E+07
20	1.99E-92	1.99E-92	2.19E+05	8.86E+07
30	8.35E-58	8.35E-58	2.33E+05	9.18E+07
40	1.89E-40	1.89E-40	2.65E+05	9.81E+07
50	5.16E-30	5.16E-30	3.18E+05	1.07E+08
75	4.82E-16	4.82E-16	5.69E+05	1.40E+08
100	5.14E-09	5.14E-09	1.10E+06	1.89E+08
125	8.95E-05	8.95E-05	2.17E+06	2.57E+08
150	6.24E-02	6.24E-02	4.30E+06	3.50E+08
175	6.86E+00	6.86E+00	8.44E+06	4.75E+08
200	2.37E+02	2.37E+02	1.64E+07	6.46E+08
225	3.78E+03	3.78E+03	3.11E+07	8.77E+08
250	3.50E+04	3.50E+04	5.80E+07	1.19E+09
275	2.18E+05	2.18E+05	1.06E+08	1.62E+09
300	1.00E+06	1.00E+06	1.87E+08	2.19E+09
325	3.68E+06	3.68E+06	3.21E+08	2.96E+09
350	1.12E+07	1.12E+07	5.35E+08	3.98E+09
375	2.97E+07	2.97E+07	8.63E+08	5.32E+09
400	6.96E+07	6.96E+07	1.35E+09	7.03E+09

Me_3PL

T(K)	TST	CVT	CVT/ZCT	CVT/SCT
6	0.00E+00	0.00E+00	NaN	NaN
8	1.12E-248	1.12E-248	6.28E-08	7.23E-01
10	9.55E-197	9.55E-197	6.28E-08	7.24E-01
20	9.05E-93	9.05E-93	1.21E-07	8.63E-01
30	5.17E-58	5.17E-58	1.12E-05	3.13E+00
40	1.40E-40	1.40E-40	1.80E-03	3.29E+01
50	4.35E-30	4.35E-30	7.56E-02	3.19E+02
75	4.73E-16	4.73E-16	2.21E+01	1.66E+04
100	5.15E-09	5.15E-09	5.95E+02	1.81E+05
125	8.60E-05	8.60E-05	5.87E+03	9.04E+05
150	5.55E-02	5.55E-02	3.42E+04	2.94E+06
175	5.57E+00	5.57E+00	1.44E+05	7.39E+06
200	1.74E+02	1.74E+02	4.89E+05	1.58E+07
225	2.51E+03	2.51E+03	1.41E+06	3.01E+07
250	2.09E+04	2.09E+04	3.59E+06	5.31E+07
275	1.18E+05	1.18E+05	8.23E+06	8.83E+07
300	4.92E+05	4.92E+05	1.73E+07	1.40E+08
325	1.64E+06	1.64E+06	3.35E+07	2.14E+08
350	4.56E+06	4.56E+06	6.09E+07	3.16E+08
375	1.10E+07	1.10E+07	1.04E+08	4.52E+08
400	2.37E+07	2.37E+07	1.69E+08	6.30E+08

$^{15}Me_3PL$

T(K)	TST	CVT	CVT/ZCT	CVT/SCT
6	0.00E+00	0.00E+00	NaN	NaN
8	2.40E-258	2.40E-258	1.55E-38	2.54E-29
10	1.86E-204	1.86E-204	2.53E-33	1.53E-25
20	1.49E-96	1.49E-96	7.41E-17	3.52E-12
30	1.51E-60	1.51E-60	4.87E-10	2.83E-06
40	1.50E-42	1.50E-42	2.01E-06	4.28E-03
50	9.17E-32	9.17E-32	3.69E-04	4.01E-01
75	2.05E-17	2.05E-17	5.70E-01	2.06E+02
100	2.87E-10	2.87E-10	3.09E+01	5.26E+03
125	5.34E-06	5.34E-06	4.23E+02	3.97E+04
150	3.64E-03	3.64E-03	2.88E+03	1.62E+05
175	3.76E-01	3.76E-01	1.30E+04	4.69E+05
200	1.20E+01	1.20E+01	4.51E+04	1.09E+06
225	1.74E+02	1.74E+02	1.30E+05	2.21E+06
250	1.47E+03	1.47E+03	3.28E+05	4.04E+06
275	8.29E+03	8.29E+03	7.40E+05	6.87E+06
300	3.48E+04	3.48E+04	1.53E+06	1.11E+07
325	1.16E+05	1.16E+05	2.92E+06	1.70E+07
350	3.24E+05	3.24E+05	5.22E+06	2.52E+07
375	7.84E+05	7.84E+05	8.81E+06	3.61E+07
400	1.69E+06	1.69E+06	1.41E+07	5.02E+07